UNCLASSIFIED

AD NUMBER
AD917091
LIMITATION CHANGES
TO: **Approved for public release; distribution is unlimited.**
FROM: **Distribution authorized to U.S. Gov't. agencies only; Test and Evaluation; OCT 1973. Other requests shall be referred to Air Force Avionics Laboratory, Attn: TEO, Wright-Patterson AFB, OH 45433.**
AUTHORITY
AFAL ltr, 20 Jan 1976

THIS PAGE IS UNCLASSIFIED

THIS REPORT HAS BEEN DELIMITED
AND CLEARED FOR PUBLIC RELEASE
UNDER DOD DIRECTIVE 5200.20 AND
NO RESTRICTIONS ARE IMPOSED UPON
ITS USE AND DISCLOSURE.

DISTRIBUTION STATEMENT A

APPROVED FOR PUBLIC RELEASE;
DISTRIBUTION UNLIMITED.

AFAL-TR-73-94
PART II

AD 917091

0.85 MICRON SOLID STATE LASER MATERIAL EVALUATION · PART II

E.P. Chicklis, R.C. Folweiler, C.S. Naiman, et al

TECHNICAL REPORT AFAL-TR-73-94, PART II

OCTOBER 1973

AD No.
DDC FILE COPY

DDC
RECEIVED
FEB 25 1974
E

DISTRIBUTION LIMITED TO UNITED STATES GOVERNMENT AGENCIES ONLY; BY REASON OF INCLUSION OF TEST AND EVALUATION DATA; APPLIED OCTOBER 1973. OTHER REQUESTS FOR THIS DOCUMENT MUST BE REFERRED TO AFAL/TEO, WRIGHT-PATTERSON AFB, OHIO 45433.

AIR FORCE AVIONICS LABORATORY – AIR FORCE SYSTEMS COMMAND
Wright-Patterson Air Force Base, Ohio 45433

NOTICE

When Government drawings, specifications, or other data are used for any purpose other than in connection with a definitely related Government procurement operation, the United States Government thereby incurs no responsibility nor any obligation whatsoever; and the fact that the government may have formulated, furnished, or in any way supplied the said drawings, specifications, or other data, is not to be regarded by implication or otherwise as in any manner licensing the holder or any other person or corporation, or conveying any rights or permission to manufacture, use, or sell any patented invention that may in any way be related thereto.

Copies of this report should not be returned unless return is required by security considerations, contractual obligations, or notice on a specific document.

AFAL-TR-73-94
PART II

0.85 MICRON SOLID STATE LASER MATERIAL EVALUATION·PART II

E.P. Chicklis, R.C. Folweiler, C.S. Naiman, et al

DISTRIBUTION LIMITED TO UNITED STATES GOVERNMENT AGENCIES ONLY; BY REASON OF INCLUSION OF TEST AND EVALUATION DATA; APPLIED OCTOBER 1973. OTHER REQUESTS FOR THIS DOCUMENT MUST BE REFERRED TO AFAL/TEO, WRIGHT-PATTERSON AFB, OHIO 45433.

FOREWORD

This is the second semi-annual report on Contract F33615-72-C-2065 and covers the work performed to evaluate the 0.85 micron solid state laser material Erbium:Yttrium Lithium Fluoride. The work on the first part of the program is described in AFAL-TR-73-94 (Part I). The first part of the series does not have a part designation.

This contract is sponsored by Advanced Research Projects Agency under ARPA Order No. 2075. The amount of the contract is $155,270. The inclusive dates of the research reported are 5 December 1972 to 5 June 1973.

Mr. Richard L. Remski (TEO), Air Force Avionics Lab, Air Force Systems Command, Wright-Patterson Air Force Base, Ohio is the Project Monitor of this program.

These studies were carried out at Sanders Associates, Electro-Optics Division, Merrimack facility. Subcontracting services were provided by the Center of Material Sciences and Engineering, Crystal Physics Laboratory, Department of Electrical Engineering, Massachusetts Institute of Technology.

Dr. C. S. Naiman, Manager - Laser Systems Department is the Project Supervisor and E. P. Chicklis and R. C. Folweiler are the principal investigators. Mr. J. C. Doherty assisted with the laser measurements and Ms. S. Lichtensteiger the spectroscopic measurements. The subcontracting efforts were directed by Dr. A. Linz. Crystals were grown by Dr. D. R. Gabbe and R. Mills. Dr. H. P. Jenssen assisted with some of the spectroscopic measurements and analyses.

The views and conclusions contained in this document are those of the authors and should not be interpreted as necessarily representing the official policies, either expressed or implied, of the Advanced Research Projects Agency or the U. S. Government.

This technical report has been reviewed and is approved.

AMOS H. DICKE, Chief
Electro-Optics Device Branch
Electronic Technology Division

ABSTRACT

This second semi-annual report describes the current status of the program for the development of a room temperature, 0.85 micron optically pumped laser material: Er:YLF. Substantial progress has been made in defining the physical, spectroscopic and laser characteristics of this material. The measured value of the stimulated emission cross section is 1.5×10^{-19} cm^2. Laser oscillations in this material are predominantly π polarized. Long pulse operation at up to 33 pps is reported. The maximum observed output power was of 0.25 watts at 11 pps from a 5.5 x 52 mm 2% Er rod.

TABLE OF CONTENTS

Section		Page
1	REPORT SUMMARY	1
1.1	Accomplishments	1
2	INTRODUCTION	3
3	CRYSTAL GROWTH	7
4	SPECTROSCOPY	11
4.1	Er^{3+} Energy Levels	11
4.1a	Wavelengths of the Laser Oscillations	11
4.2	Stimulated Emission Cross Section for the .8052 μm Laser Transition in Er:YLF	13
4.3	Quenching of the Terminal Level	19
4.4	Effects of Long Terminal Level Lifetime	19
4.4.1	Inversion Saturation in Repetitively Pulsed Operation	21
4.4.2	Depopulation of the Ground Level	21
4.4.3	Inversion Reduction: Single Shot	21
4.4.3.1	Threshold Condition	22
4.4.3.2	Two Level Laser - No Fluorescence	23
4.4.3.3	Effects of Terminal Manifold Splitting	24
4.4.3.4	Effects of Fluorescence - Non-radiative Decay	24
4.4.3.5	An Example	26

TABLE OF CONTENTS (Cont)

Section		Page
5	LASER MEASUREMENTS	29
5.1	Single Shot Data	29
5.1.1	Rod 446.1a 2% Er: 5.5 x 52 mm	29
5.1.2	Rod 448 2%Er - 1% Tm	34
5.2	Repetitively Pulsed Data	34
5.2.1	Rod 446.2, 2% Er (3 x 23 mm)	36
5.2.2	Rod 446. 1a, 2% Er, 5.5 x 52 mm	37
5.3	Laser Polarization and Q-Switching	40
5.3.1	Polarization	40
5.3.2	Q-Switching	40
	REFERENCES	43/44
	APPENDIX I - Strength Measurement	45

LIST OF TABLES

TABLE		PAGE
I	Physical & Mechanical Properties of YLF	4
II	Possible Laser Transitions at 0.8502 ± 0.0002μm	13
III	Upper and Lower Level Lifetimes of Er:YLF	20
A-I	Strength of αβYLF	47/48

LIST OF ILLUSTRATIONS

FIGURE		PAGE
1	Level Diagram of Er^{3+}:YLF	12
2	Er:YLF Emission Spectrum	14
3	Er:YLF Absorption $^4I_{15/2} \rightarrow {}^4S_{3/2}$	17
4	0.85μm Long Pulse Input/Output	30
5	Threshold vs. Mirror Reflectivity	35
6	Single Shot Input/Output	39

1.0 REPORT SUMMARY

The results of the second six months of an eighteen month program to investigate the physical, spectroscopic, and laser properties of Er^{3+}:$LiYF_4$(YLF) are presented. Laser oscillations at 0.85 μm are obtained in this optically pumped solid state material as the result of stimulated $^4S_{3/2}$ - $^4I_{13/2}$ transitions in the Er^{3+} ions.[1,2] The objectives of this program are:

a. Measurement of pertinent thermal and mechanical properties of this material.

b. Measurement of spectroscopic properties of interest with particular attention to quenching of the terminal state lifetime.

c. Measurement of the laser operating characteristics of 5 x 50 mm laser rods with particular attention to average power capabilities at 20 - 30 Hz.

1.1 ACCOMPLISHMENTS

The major accomplishments during this phase of the program include:

I. Laser Operation: 2% Er:YLF

The maximum power observed in a 5.5 x 52 mm rod was 0.25 watts (11 Hz); the average output power under these conditions approximately equalled the single shot output energy times repetition rate. The maximum repetition rate observed was 33 Hz. In a 3 x 23 mm rod 40 mW was obtained at 20 Hz with 320 watts input. Q switched operation of a 3 x 23 mm rod was obtained (KDP/Calcite) with and without the polarizing element.

II. Polarization, Wavelength of Oscillations and Beam Divergence

The measured wavelength of laser oscillations at 2 x threshold in a 3 x 23 mm rod operated at 5 Hz was

$$\lambda = 0.8502 \pm 0.0002 \ \mu m.$$

Laser oscillations are π polarized; however, as the emission spectrum exhibits a σ line ($\pi/\sigma \simeq 2.5$) a polarizing element in the resonator may be required at high inversion. Estimates of the beam divergence, visually determined with an image converter, are between 1 - 2 mr with no apparent increase with average power loading.

III. Spectroscopic Analysis for Laser Optimization

The stimulated emission cross section was measured by the method of Kushida et al. and found to be

$\sigma = 1.5 \times 10^{-19} cm^2$ for the π polarized line. Investigation of means to quench the terminal level lifetime using samples co-doped with Tm^{3+} and Pr^{3+} are summarized. With as little as 1% Pr added to a 2% Er crystal the terminal level is quenched by a factor of 35 (lifetime < 400 μs).

2.0 INTRODUCTION

Laser operation at 0.85 μm is obtained in Er^{3+}:YLF[1,2] via stimulated $^4S_{3/2} \rightarrow {}^4I_{13/2}$ transitions in this optically pumped material. YLF ($LiYF_4$) is a fluoride host of the tetragonal Scheelite structure ($CaWO_4$) with a c/a ratio of 2.08. Crystals of arbitrary amounts of Er^{3+} substituted for the Y^{3+} site can be grown (up to $LiErF_4$).

YLF crystals are grown by the Top Seeded Solution technique [3] from a LiF rich melt in an inert atmosphere (He). A detailed account of the growth technique is presented in (4,5). The physical and mechanical properties of YLF measured on this and other programs are presented in Table I for reference.

Interest in the development of an optically pumped solid state laser material at .85 microns stems from the potential of obtaining a source of very high brightness in a nonvisible wavelength region for which excellent point and imaging detectors have been developed. The feasibility of an Er^{3+}:YLF laser system must be evaluated in the context of the performance capabilities of such a system compared to that attainable using existing sources.

Although a complete systems analysis is not an appropriate part of this program, it is instructive to consider approximate laser performance goals for this material with which a competitive systems capa-

TABLE I

PHYSICAL PROPERTIES OF $LiYF_4$ (YLF)

MECHANICAL	YLF
Density (gm/cm^3) (undoped)	3.99
αβYLF	5.07
Hardness (Moh)	4-5
Elastic Modulus (N/m^2)	7.5×10^{10}
Poissons Ratio	0.33
Strength (Modulus of Rupture, Kg/cm^2)	335
THERMAL (300°K)	
Thermal Conductivity (W/cm - °K)	0.06
Thermal Expansion Coefficient -($°C^{-1}$) 0-100°C	a axis : 13.8×10^{-6} c axis : 9.0×10^{-6}
OPTICAL	
Index of Refraction (λ = 0.6 μm)	$N_o = 1.443$ $N_e^o = 1.464$
UV Absorption	<0.2μm
CRYSTALLINE STRUCTURE	Tetr. (Scheelite)
a - axis (Å)	5.167
c - axis (Å)	10.735
c/a ratio	2.078

bility appears attainable. Three cases are distinguished:

(a) Peak Power

Applications for high peak power sources include range finders and target designators. The source/detector combination for the former is Nd:YAG/Si Avalanche and for the latter Nd:YAG/Si Quadrant. At 0.85 μm Si detectors (avalanche and quadrant cells) are superior by about a factor of three in sensitivity[6] and considerably lower in cost.[7]

Neglecting the somewhat higher background radiance of the sun at 0.85 μm and the slightly higher scattering coefficient ($\sigma.85/\sigma1.06 \sim 1.1$[8]), roughly 1/3 the transmitted peak power is required at 0.85 compared to 1.06 for equivalent systems performance.

(b) Average Power

Applications which require average power generally involve imaging systems (gated active viewing, for example). Because of the poor imaging capabilities at 1.06 μm (S-1 responsivity $\simeq 4 \times 10^{-4}$ amps/watt), Nd:YAG systems are impractical. Instead GaAs diode arrays cooled to 77°K ($\lambda \simeq 0.85$ μm) are utilized in conjunction with extended red S-20 surfaces (responsivity $> 10^{-2}$ amps/watt). Such arrays are capable of radiating $\simeq$ 30 watts into a 3° FOV[9], corresponding to an irradiance of 1.4×10^4 watts/ster. The same target irradiance can be obtained with 1 mr FOV utilizing Er^{3+}:YLF with only 12 mW transmitted.

(c) Energy

Applications which require only energy in a single pulse are restricted to photographic systems. Use of Er^{3+}:YLF for active, covert photography presents substantial improvement over GaAs. Because of the relatively large amount of energy in a short pulse available in Er^{3+}:YLF, short exposure times in photographic systems can be obtained.

3.0 CRYSTAL GROWTH

A rather extensive description of the growth technique employed for obtaining the YLF crystals utilized in this program is discussed in Technical Report AFAL-TR-73-94 entitled "0.85 Micron Solid State Laser Material Evaluation." During this period the following crystals were grown.

Sample No.	M.I.T. No.	Composition	Size
454	196f	1% Er: 0.5% Pr	Spectroscopic
450	191f	1% Er: 2% Pr	Spectroscopic
449	190f	1% Er	Spectroscopic
448	178f	2% Er - 1% Tm	5.5 x 5.5 x 54 mm

In this report we will present some aspects of the problem of obtaining high optical quality crystals. The types of defects observed are bubbles associated with a core and a fine precipitate. It must be emphasized that the presence of these defects at the density normally present does not prevent laser action, nor have we found any correlation between the presence of these inclusions and the susceptibility of the material to Q-switched damage.

It is believed that the bubbles are He gas exsolved from the melt. Bubble formation is probably assisted through nucleation on an impurity

site or other melt disturbance and trapped on the slightly concave crystal melt interface. We have recently changed over to use of high purity Ar (99.9995%) now commercially available from Matheson and other suppliers at a reasonable cost) which is less soluble than He in the fluoride melt, and therefore should yield crystals with a lower bubble density if exsolution of gas is a contributing factor. Evaluation of Ar as the furnace ambient is not complete and its effect on bubble size and density is not yet known.

Attempts have been made to analyze the core material of the bubbles using the electron microprobe. Results to date have been inconclusive in terms of identifying specific elements concentrated in the inclusion. However, the results have indicated the presence of trace K, Ca, Ba, Na, Mg, Si, in both the inclusion and bulk material. The electron microprobe data at this point is only qualitative, agreeing in this sense with mass spectrographic analysis reported earlier.

The fine precipitate has not been adequately characterized. Possibilities are that it is colloidal to submicron in size and sometimes oriented as suggested by its appearance when viewed by scattered light. Formation of a precipitate certainly requires an impurity to be present and often two. For example, in sodium fuoride an oxide-bearing precipitate will not form at concentrations outside the fluoride solubility limit unless an impurity such as magnesium is also present. In other words, in the polycomponent system $LiF\text{-}YF_3\text{-}Y_2O_3\text{-}MF_x$, where M is an impurity metal ion and x reflects its valence, the <u>solid</u> phase M_aO_b will exist in equilibrium with solid $LiYF_4$ at extremely low M and $O^=$ concentrations. The law of mass action applies; increasing either the M or O concentration will drive the system towards formation of a

precipitate. In the absence of the offending metallic impurity, the precipitate will not form. Equilibration and precipitation in the solid phase are reached slowly and only above a characteristic temperature. We have observed the following behavior in the development of traces of a precipitate in YLF. The small boule grown to clean the melt surface which is grown (pulled) at a higher rate (about 5mm/hour) than the laser crystal is not affected by precipitation. Annealing of this clear material close to the melting point results in the formation of a precipitate. The annealing experiments are incomplete, but lead to the idea that at the crystal growth rates used some precipitation can occur in the hot crystal just behind the melt-solid interface. The effect of an increased growth rate is to shorten the time the material spends above the characteristic temperature, thereby limiting the amount of precipitation which can take place. The use of higher growth rates (1.5 mm/hour as opposed to the 1 mm/hour commonly used) is being investigated in an attempt to minimize the precipitation phenomenon without entering a region of high growth rate-related defect formation.

4.0 SPECTROSCOPY

Spectroscopic measurements were made in order to determine the stimulated emission cross section of the laser transition. Quenching of the terminal level lifetime with Pr^{3+} was investigated and an analysis of the effects of the long terminal lifetime on laser operation conducted.

4.1 Er^{3+} ENERGY LEVELS

The positions of the pertinent Er^{3+} levels were determined by low temperature (4.2°K) absorption and emission spectra in order to identify the participating levels of the laser transition. Positions of these levels ($^4S_{3/2}$, $^4I_{13/2}$, $^4I_{15/2}$) are tabulated in Figure 1. Note that the positions of the $^4I_{13/2}$ and $^4I_{15/2}$ levels differ from those reported by Brown, et al.[10] by some 25 cm^{-1}.

4.1a WAVELENGTHS OF THE LASER OSCILLATIONS

Measurements of the emission wavelength were made using a SSR Optical Multichannel Analyzer (OMA) and verified with a Jarrell Ash 1/2 meter grating monochromator (590 ℓ/mm). The laser was operated at 5 pps at ∿ 2 x the threshold energy. The OMA provided a real time display in 500 channels, with a resolution of 5 A°/channel. Only one laser line centered at 0.85 μm was observed with this instrument.

YLF : Er

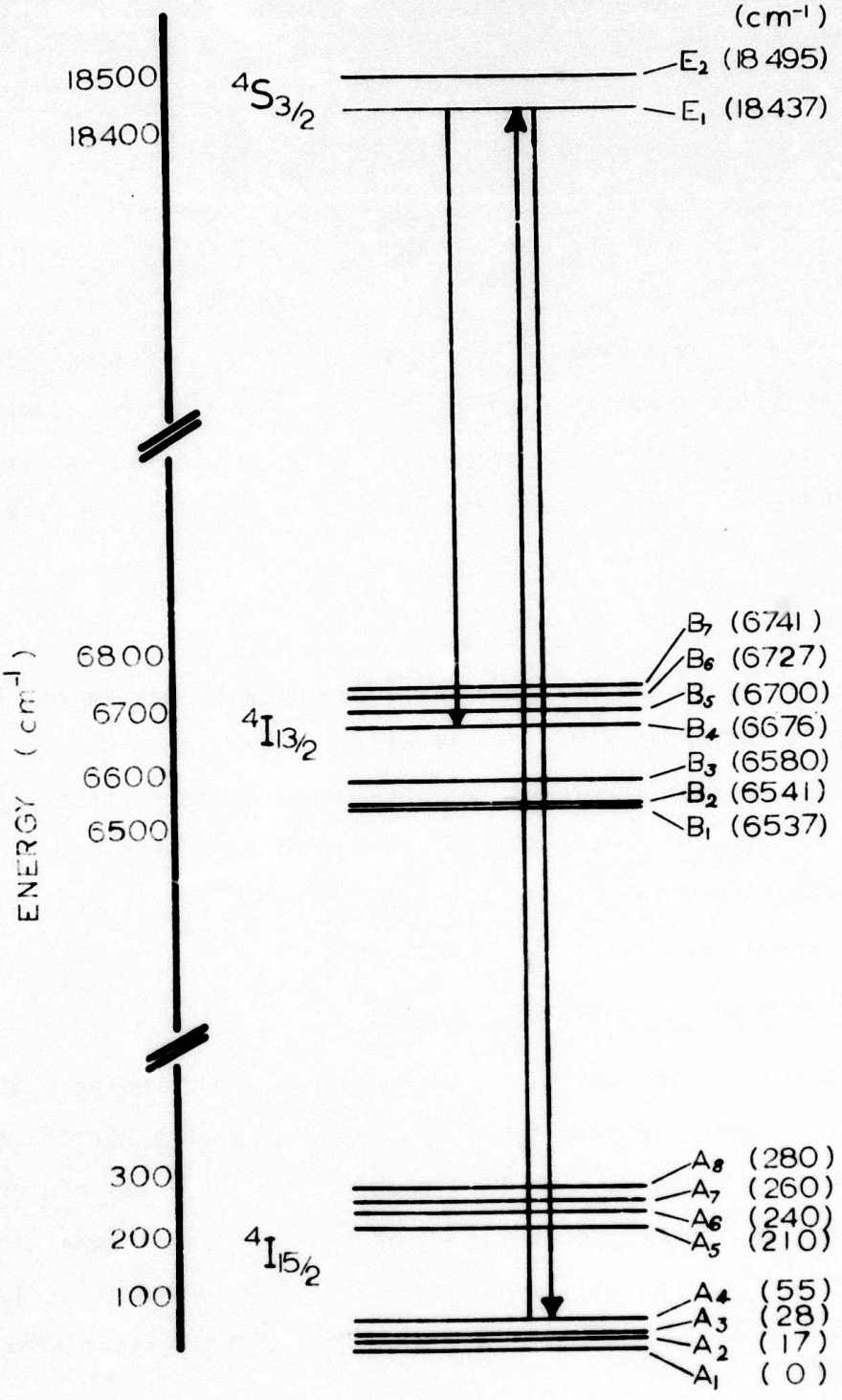

Figure 1
Energy Level Diagram

D-82

More careful measurement of the oscillation was made with the Jarrel Ash manually scanned in the region of interest. The wavelength of the emission was found to be

$$\lambda = 0.8502 \pm 0.0002 \ \mu m$$

with the observed linewidth of the emission instrument limited. This corresponds to the center of the fluorescence line strongest in the π spectrum (Figure 2). From the level positions at 4.2°K (Table II), three possible transitions can be identified within the room temperature linewidth of the .8502 μm peak identified in Table II.

TABLE II

POSSIBLE LASER TRANSITIONS at .08502 ± 0.0002 μm

TRANSITION	WAVELENGTH AT LINE CENTER *
$E_1 \rightarrow B_4$	0.8504 ± 0.0003
$E_2 \rightarrow B_6$	0.8497 ± 0.0003
$E_2 \rightarrow B_7$	0.8507 ± 0.0003

*Determined from low temperature (4.2°K) fluorescence; the line center shift at room temperature is believed to be small.

4.2 STIMULATED EMISSION CROSS SECTION FOR THE .8052 μm LASER TRANSITION IN Er:YLF

Basically the method of measuring the cross section for a four level laser is:

1. Measure absorption cross section from ground state to upper laser level (σ_a). This cross section is equal to stimulated emission cross section for tran-

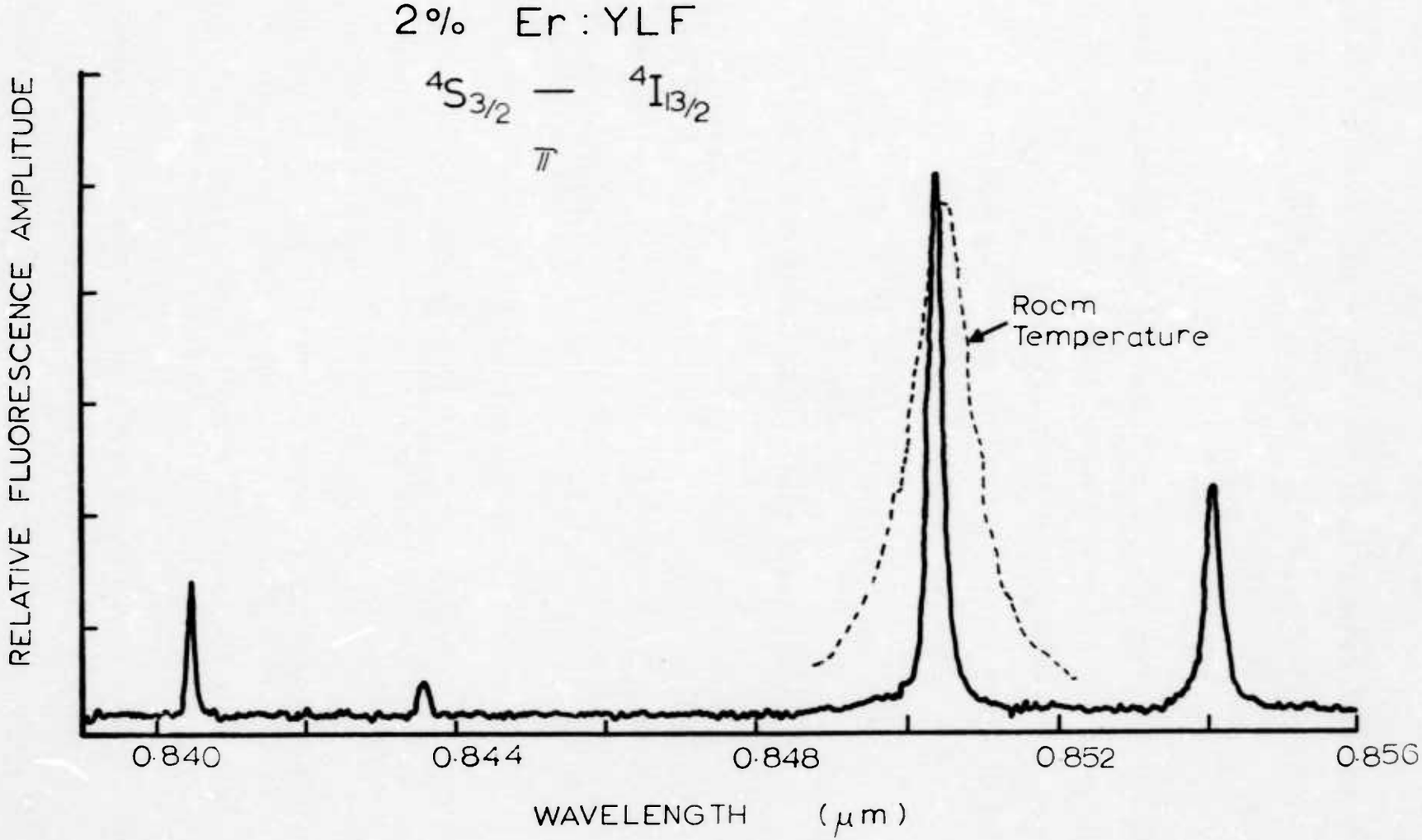

Figure 2
4.2°K EMISSION SPECTRUM

sition from upper laser level to ground state -- provided the level degeneracies are the same.

2. Measure ratio of the intensities of laser line and transition of known cross section: I_ℓ / I_a

3. We then have[11]:

$$\frac{I_\ell}{I_a} = \left(\frac{\lambda_a}{\lambda_\ell}\right)^3 \frac{\sigma_\ell}{\sigma_a}$$

$$\text{or} \quad \sigma_\ell = \sigma_a \frac{I_\ell}{I_a} \left(\frac{\lambda_\ell}{\lambda_a}\right)^3$$

which is valid for the .85 μm laser transition in Er^{3+}:YLF as the levels in $^4S_{3/2}$ and $^4I_{13/2}$ and $^4I_{15/2}$ are all doubly degenerate.

The positions of the energy levels of the Er^{3+}: $^4I_{15/2}$, $^4I_{13/2}$ and $^4S_{3/2}$ manifolds are shown in Figure 1. The laser transition is the $E_1 \rightarrow B_4$ transition at .8502 μm. Also the $E_2 \rightarrow B_6$ at .8497 μm and the $E_2 \rightarrow B_7$ at .8507 μm are close enough that they would contribute, but they seem to be much weaker than the $E_1 \rightarrow B_4$ transition. In order to estimate the cross section of the $E_1 \rightarrow B_4$ transition, use is made of the $A_4 \rightarrow E_1$ absorption transition. This transition is observed in both absorption and fluorescence at room temperature and is well separated from other lines. Also, since the strongest emission at .8502 μm is π-polarized, only the cross section for the π-polarized light will be considered.

Figure 3 shows the $^4I_{15/2} \rightarrow {}^4S_{3/2}$ polarized absorption spectrum at room temperature. The $A_4 \rightarrow E_1$ transition is indicated by an arrow. The peak absorption coefficient (α) for this line is 0.83 cm^{-1}. The Er ion density is $2.65 \times 10^{20} cm^{-3}$ for 2% concentration.[+] The absorption cross section is simply the absorption coefficient per atom obtained from α and the population of the lower level. At room temperature the A_4 population density is obtained from

$$N_{A_4} = N_0 \frac{g \exp^{-E_{A_4}/kT}}{Z}$$

where Z is the partition function of $^4I_{15/2}$ at room temperature, and g is the level degeneracy of A_4 (=2):

$$Z = \Sigma_i g_i \exp(-E_i/kT)$$
$$= 9.6$$

then

$$N_{A_4} = 2.65 \times 10^{20} \times \frac{2 \exp(-55/208)}{9.6}$$

$$N_{A_4} = 4.24 \times 10^{19} \text{ cm}^{-3}$$

from which we obtain the absorption cross section

$$\sigma_A = \frac{\alpha}{N_{A_4}} = 1.95 \times 10^{-20} \text{ cm}^2$$

To find the emission cross section for the 8502 Å line, the ratio of the fluorescent intensity of the $E_1 \rightarrow A_4$ and the $E_1 \rightarrow B_4$ lines were measured. A spectroscopic sample with 1/2% Er was used to minimize the radiation trapping of the

[+] Er^{3+} concentration in the melt

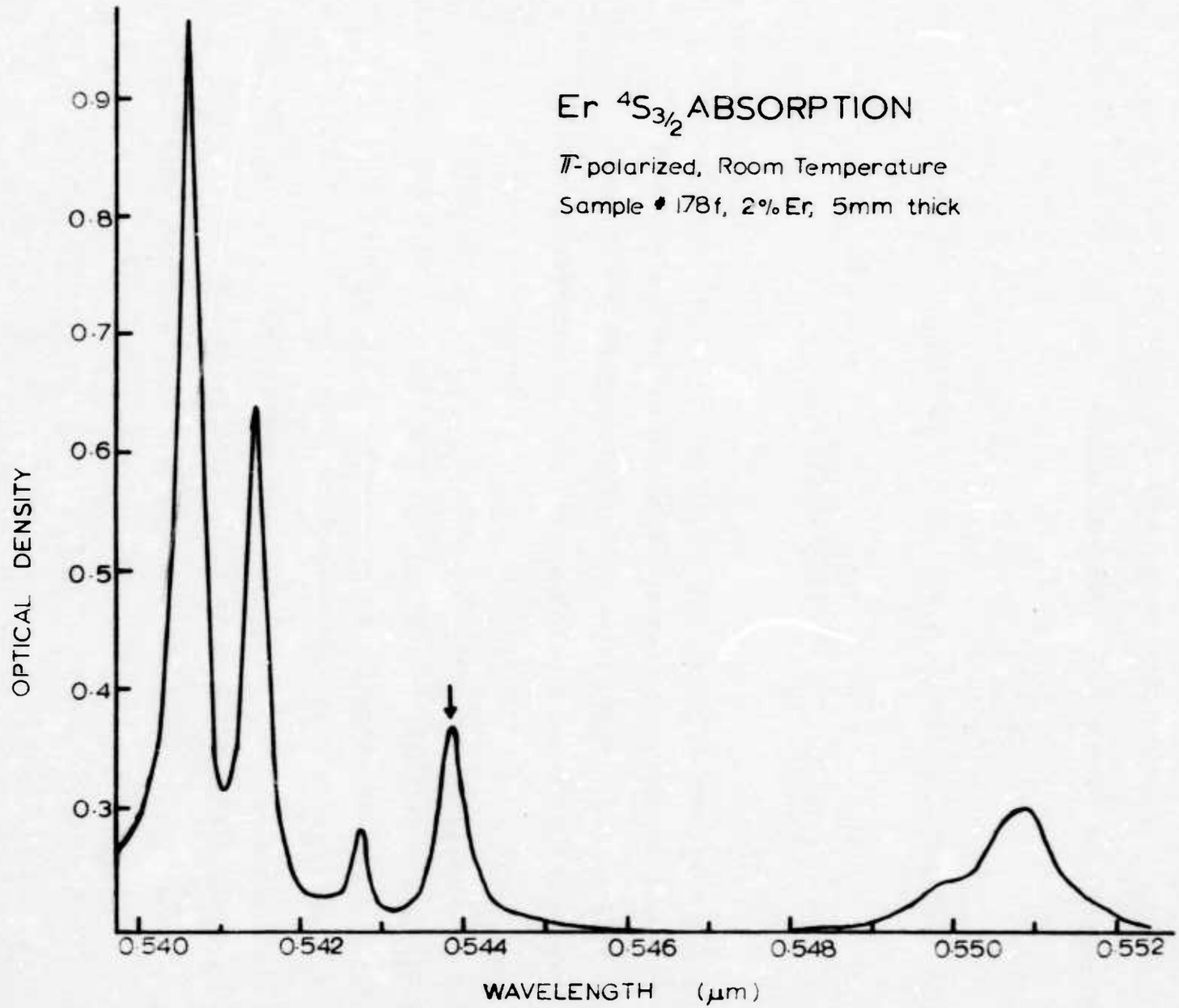
Er $^4S_{3/2}$ ABSORPTION
π-polarized, Room Temperature
Sample # 178f, 2% Er, 5mm thick
OPTICAL DENSITY
0.9
0.8
0.7
0.6
0.5
0.4
0.3
0.540
0.542
0.544
0.546
0.548
0.550
0.552
WAVELENGTH (μm)
D-81

Figure 3
17

$E_1 \rightarrow A_4$ fluorescence. The detection system was calibrated for relative response versus wavelength with the use of a calibrated DXW 1000 W lamp. The result was:

$$\frac{I\ (E_1 \rightarrow B_4)}{I\ (E_1 \rightarrow A_4)} = 2.0$$

The stimulated emission cross section for the laser line is then:

$$\sigma_\ell = \sigma_A \times \left[\frac{\lambda(E_1 \rightarrow B_4)}{\lambda(E_1 \rightarrow A_4)}\right]^3 \times \frac{I(E_1 \rightarrow B_4)}{I(E_1 \rightarrow A_4)} = 1.5 \times 10^{-19} cm^2$$

in π polarization.

The experimental uncertainties in the emission cross section measurement include contributions from the determination of the absorption cross section ($A_4 \rightarrow E_1$) and the fluorescence branching ratio. The former measurement is believed accurate to within 5%, the sources of error being the A_4 level population and the optical density measurement. The fluorescence branching ratio measurement utilized a calibrated tungsten lamp for which the relative radiance between 0.85 μm and 0.55 μm is known to be better than 5%.

A larger potential source of error arises from possible contributions from the $E_2 \rightarrow B_6$ and $E_2 \rightarrow B_7$ transitions whose line centers fall within the linewidth of the room temperature emission centered at .8502 μm. Emission spectra at 4.2°K (where the E_2 population is negligible) and above revealed a gradual broadening of the emission without evidence of additional structure with temperature. The extent of the line broadening from 4.2 to 300 °K was similar to the increased

width of other lines. Thus, the two E_2 transitions appear to be very weak and were not included in the σ calculation.

In conclusion, the stimulated emission cross section for the $E_1 \rightarrow A_4$ transition in Er^{3+}:YLF is

$$1.5 \pm 0.2 \times 10^{-19} \text{ cm}^2$$

in π polarization (parallel to the C axis).

4.3 QUENCHING OF THE TERMINAL LEVEL

In an earlier report [5] the effects of co-doping with Tm^{3+}, Ho^{3+}, Tb^{3+} and Pr^{3+} on the terminal level ($^4I_{13/2}$) were described. Table III shows the effects of co-doping on the lifetimes of interest. It is seen that only Pr in concentrations of $\simeq$ 1% yields the desired effect, viz. reduction of the terminal level lifetime without serious degradation of the storage time of the upper laser level ($^4S_{3/2}$).

The pertinent lifetimes of samples of lower Er concentration are also presented in Table III. Quenching factors for $^4I_{13/2}$ were obtained by comparison of the $^4I_{11/2}$ and $^4I_{13/2}$ amplitudes in a singly doped reference sample (Er:YLF) to that of the multiply doped sample.

4.4 EFFECTS OF LONG TERMINAL LEVEL LIFETIME

Although the $^4I_{13/2}$ lifetime can be substantially reduced by the addition of Pr^{3+}, it does not appear possible to quench this level so that its decay rate is comparable to the pumping rate of the level in Q switched operation. There are at least three potential problems associated with a long terminal level lifetime:

TABLE III

UPPER AND LOWER LEVEL LIFETIMES OF ER:YLF

Sample Number	Composition	Quenching Factor $^4I_{13/2}$	$^4I_{13/2}$ Lifetime (ms)	$^4S_{3/2}$ Lifetime (μs)
391	2% Er	--	13 ± 1	200 ± 20
442	2% Er-1% Tm	11	1.1*	90 ± 20
439	2% Er-2% Tm	18	0.7*	70 ± 20
444	2% Er-1% Pr	35	0.4*	170 ± 20
445	2% Er-2% Pr	50	0.25*	110 ± 20
411	2% Er-2% Tb	7	1.8	120 ± 20
436	2% Er-2% Ho	6.5	2	155 ± 20
449	1% Er	--	13 ± 1	350 ± 25
450	1% Er-2% Pr	50	0.25*	250 ± 25
458	2% Er-0.5% Pr	> 30	<0.4*	225 ± 25

* Inferred from fluorescence amplitude measurements, estimated accuracy to within a factor of 2.

4.4.1 INVERSION SATURATION IN REPETITIVELY PULSED OPERATION

At 33pps the interval between pulses is ≃ 30ms; between pulses the level decays by exp (-3), or to 0.05 of the initial value. Addition of very small amounts of Pr, say 0.5%, provides for complete de-excitation of the level between pulses. Note, however, that operation at 33pps has been demonstrated in 2% Er:YLF without evidence of terminal level population buildup.

4.4.2 DEPOPULATION OF THE GROUND LEVEL

In the ideal case all excited levels would exhibit lifetimes much shorter than the flashpulse duration except for the upper laser level (Nd:YAG, for example). Then during the flashpulse all excited ions either feed the upper level or recycle to the ground level. In Er:YLF $^4I_{11/2}$ and $^4I_{13/2}$ are very long lived (≃ ms lifetimes); ions which are pumped to these levels by the flashlamp or by non-radiative decay cannot be utilized. The result is an effective decrease in the active ion density available for pumping, the effects of which on laser operation are not yet known.

4.4.3 INVERSION REDUCTION: SINGLE SHOT

In single shot output the population of the terminal laser manifold, $^4I_{13/2}$, increases with each stimulated or spontaneous transition to that level. In experiments with the $^4S_{3/2}$ - $^4I_{13/2}$ laser transition in $Er^{3+}:YAlO_3$ Weber[12] observed saturation of the 0.85 μm laser output in 1% Er rods at only a few mJ output. This was attributed to sufficient population buildup of the long lived (~5ms) terminal level in this host to quench the inversion.

This effect has not been observed in Er^{3+}:YLF. Up to 150 mJ has been extracted from a 5 x 30 mm 2% Er rod in long pulse[1]. It is shown below that as a result of the terminal level splitting and the relatively slow pumping rate of $^4I_{13/2}$ in the absence of lasing, the long lived terminal level has a negligible effect on the extractable energy in Er:YLF.

4.4.3.1 Threshold Condition

The well known threshold condition for a laser oscillator[13]

$$R \exp 2\ell (\alpha - \delta) = 1, \quad \alpha = \Delta N\sigma$$

can be written as

$$\Delta N^T = \frac{-\ln R}{2\ell\sigma} + \delta/\sigma$$

where

R = coupling mirror reflectivity

ℓ = rod length

δ = loss/cm

σ = stimulated emission cross section for the laser transition = 1.5×10^{-19} cm^2

ΔN^T = population inversion required at threshold

For ℓ = 50 mm, R = 70%, δ = 1%/cm

$$\Delta N^T = 2.9 \times 10^{17} \text{ cm}^{-3}$$

between the upper and lower laser levels to maintain laser oscillations.

4.4.3.2 Two Level Laser - no Fluorescence

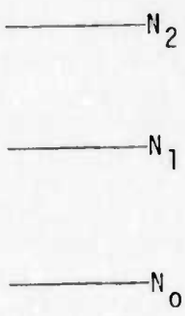

We assume N_2 is pumped above threshold and all the transitions out of N_2 are stimulated (i.e. no fluorescence). Furthermore, we assume N_1 also has an infinite lifetime. Let n denote the number of $N_2 \rightarrow N_1$ transitions. Since each transition reduces the inversion by 2 we have

$$\Delta N^f = \Delta N^i - 2n$$

where

ΔN^f (and) ΔN^i are the final and initial inversions after n transitions. Thus the number of stimulated transitions is simply

$$n = \frac{\Delta N^i - \Delta N^f}{2}$$

Laser oscillations can occur between these two levels until

$$\Delta N^f = \Delta N^T$$

Thus in the case of an infinite terminal level lifetime of a singlet lower manifold only 1/2 the inversion above the threshold inversion can be extracted. For a very rapid terminal level lifetime each transition decreases the inversion by 1 and the full excess inversion can be extracted, $n = \Delta N^i - \Delta N^T$.

4.4.3.3 Effects of Terminal Manifold Splitting

Figure 1 shows the position of the initial and final laser levels in the $^4S_{3/2}$ and $^4I_{13/2}$ manifolds. Note that the terminal level of the transition resides some 139 cm^{-1} above the lowest level of the first excited manifold. The partition function of the manifold at room temperature, Z, is 4.5 and the occupation factor of the terminal laser level (B_4) is (neglecting the common two-fold level degeneracies)

$$\frac{\exp(-139/207)}{Z} = 0.11$$

Now the thermal relaxation time between levels in the manifold is much faster than the time frame of normal mode or non-mode locked Q switched pulses. As a result thermalization is assured during oscillation. Then for every stimulated transition the terminal level (B_4) population increases by 0.11. For each transition n the change in inversion between the laser levels (assuming singlet upper manifold) is

$$\Delta N^T = \Delta N^i - 1.11n$$

or

$$n = \frac{\Delta N^i - \Delta N^T}{1.11}$$

Thus 90% of the initial excess inversion is extracted as laser output independent of the pumping level above threshold.

4.4.3.4 Effects of Fluorescence - Non-radiative Decay

In addition to the buildup of the terminal level population due to stimulated transitions, the effects of fluorescence and non-radiative decay must be considered. Population buildup in $^4I_{13/2}$ is due to

non-radiative decay by multiphonon relaxation, $^4S_{3/2}$ - $^4I_{13/2}$ fluorescence, and $^4S_{3/2}$ concentration quenching. Multiphonon relaxation from states between $^4S_{3/2}$ and $^4I_{13/2}$ can be neglected as the cascade is very slow due to the $^4I_{11/2}$ intermediate state which has a 4.3ms lifetime. The radiative lifetime of $^4S_{3/2}$ is some 600μs (inferred from 4.2°K lifetime measurement in 0.5% Er) for all transitions. Since the $^4S_{3/2} \rightarrow {}^4I_{13/2}$; $^4I_{15/2}$ branching ratio is <1, the $^4S_{3/2}$ - $^4I_{13/2}$ radiative rate is probably less than 10^3/sec. That is, the upper limit for $^4I_{13/2}$ pumping due to fluorescence is $\simeq 10^3$ sec^{-1} neglecting transitions from $^4F_{9/2}$, $^4I_{9/2}$(weak), $^4I_{11/2}$ (very slow), and all states above $^4S_{3/2}$ (most of which rapidly relax non-radiatively to $^4S_{3/2}$). However, the fluorescence lifetime of $^4S_{3/2}$ at room temperature in 2% Er:YLF is $\simeq$ 200μs due to $^4S_{3/2}$ concentration quenching. The mechanism for Er quenching is believed to be

$$^4S_{3/2} \rightarrow {}^4I_{13/2},\ {}^4I_{15/2} \rightarrow {}^4I_{9/2}$$

and/or

$$^4S_{3/2} \rightarrow {}^4I_{9/2},\ {}^4I_{15/2} \rightarrow {}^4I_{13/2}.$$

In either case $^4I_{13/2}$ is pumped at 1/2 the rate of this process (as the cascade from $^4I_{9/2}$ can be neglected due to the long lived $^4I_{11/2}$) or $\omega \simeq 2.5 \times 10^3$ sec^{-1}.

We can compute the population buildup due to non-radiative decay in the time frame of laser oscillations. We assume a fast flash pulse which provides some initial population N^i in the presence of the $^4S_{3/2}$ decay rate. Then the number of transitions per second from $^4S_{3/2}$ to $^4I_{13/2}$ is

$$\frac{dN}{dt} = -\omega N(t), \quad \omega = 2.5 \times 10^3 \text{ sec}^{-1}$$

or

$$N(^4S_{3/2}) = N^i e^{-\omega t}$$

and

$$N(^4I_{13/2}) = N^i (1 - e^{-\omega t})$$

But the occupation factor of the terminal level of the laser transition is 0.11 of the $^4I_{13/2}$ population, so

$$N_\ell(t) = 0.11\, N^i (1 - e^{-\omega t})$$

where N_ℓ = population density of the lower laser level. Then

$$\Delta N(t) = N(^4S_{3/2}) - N_\ell = N^i [1.11e^{-\omega t} - 0.11]$$

due to fluorescence and non-radiative decay.

4.4.3.5 An Example

We consider a 2% Er: YLF rod pumped with a Xe flashlamp appropriately filtered (water) to prevent direct pumping of $^4I_{13/2}$. The terminal level population will rise due to non-radiative decay at a rate $\omega = 2.5 \times 10^3$ until oscillations begin; thereupon the pumping rate due to fluorescence can be neglected. In this case the initial population is provided instantaneously and lasing held off for some time τ. The number of possible stimulated transitions/unit volume is

$$n = \frac{\Delta N(\tau) - \Delta N^T}{1.11}$$

where

$$\Delta N(\tau) = N^i [1.11e^{-\omega\tau} - 0.11]$$

is the inversion at the threshold for oscillations. Now the active ion density in a 2% Er:YLF rod is $N_o \simeq 3 \times 10^{20}$ ions/cm^3; the required inversion for oscillation (see 4.4.3.1) is $\Delta N^T = 2.9 \times 10^{17}$ ions/cm^3. Let us assume the material is initially pumped at 5 x threshold or $N^i = 1.5 \times 10^{18}$/cm^3, and Q switched at $\tau = 50\mu s$. Then the initial inversion at the onset of oscillation is

$$\Delta N(\tau) = 0.87\ N^i$$

and the number of stimulated transitions/cm^3 is

$$n = \frac{\Delta N(\tau) - \Delta N^t}{1.11}$$

$$= \frac{(0.87)\ 1.5 \times 10^{18} - 3.7 \times 10^{17}}{1.11}$$

$$= 0.9 \times 10^{18} cm^{-3}$$

corresponding to 0.2 joules/cm^3 at $\lambda = 0.85\mu m$.

In the case of an infinitely fast terminal level decay, under the same conditions:

$$n = \Delta N(\tau) - \Delta N^T$$

and $$\Delta N\ (\tau) = N^i e^{-\omega\tau}$$

or $$n = 1 \times 10^{18} cm^{-3}$$

corresponding to 0.23 joules/cm^3.

In the example cited approximately 0.5 joules are available in a 1/4 x 3 inch rod Q switched 50μs after a very short flash pulse pumps the material to 5 x the threshold inversion. At 10 x threshold this would be ≃ 1 joule from a 1/4 x 3 inch rod. Whether or not other factors will limit the extractable energy in Q switched operation is

not yet clear. However, the effects of the long terminal level lifetime have been shown to be negligible under these (reasonable) assumptions in single shot operation.

5.0 LASER MEASUREMENTS

The focus of the laser measurements was to demonstrate repetitively pulsed operation and to determine the average power capabilities of reasonably sized laser rods. In addition the polarization of the output and preliminary Q switched data are reported.

5.1 SINGLE SHOT DATA

5.1.1 ROD 446.1a: 2% Er: 5.5 x 52 mm

Figure 4 shows the long pulse input/output characteristics using the following pump conditions:

Flashlamp: ILC 3 x 30 mm 3000 Torr Xe

Capacitor Bank: 50 μf, 22 μH, critically damped

Resonator: Plane parallel external mirrors, rod uncoated

Note that only 30 mm of the rod was pumped. The computed slope efficiencies are:

97%R: 0.24%
70%R: 0.4%

In a separate experiment an estimate of the scattering loss of this rod was obtained using the method of Findlay and Clay [13,14] somewhat modified to account for direct flashlamp pumping of the terminal level. The threshold condition for any laser oscillator can be expressed as

$$R_1 R_2 \exp 2\ell (\alpha - \Delta) = 1$$

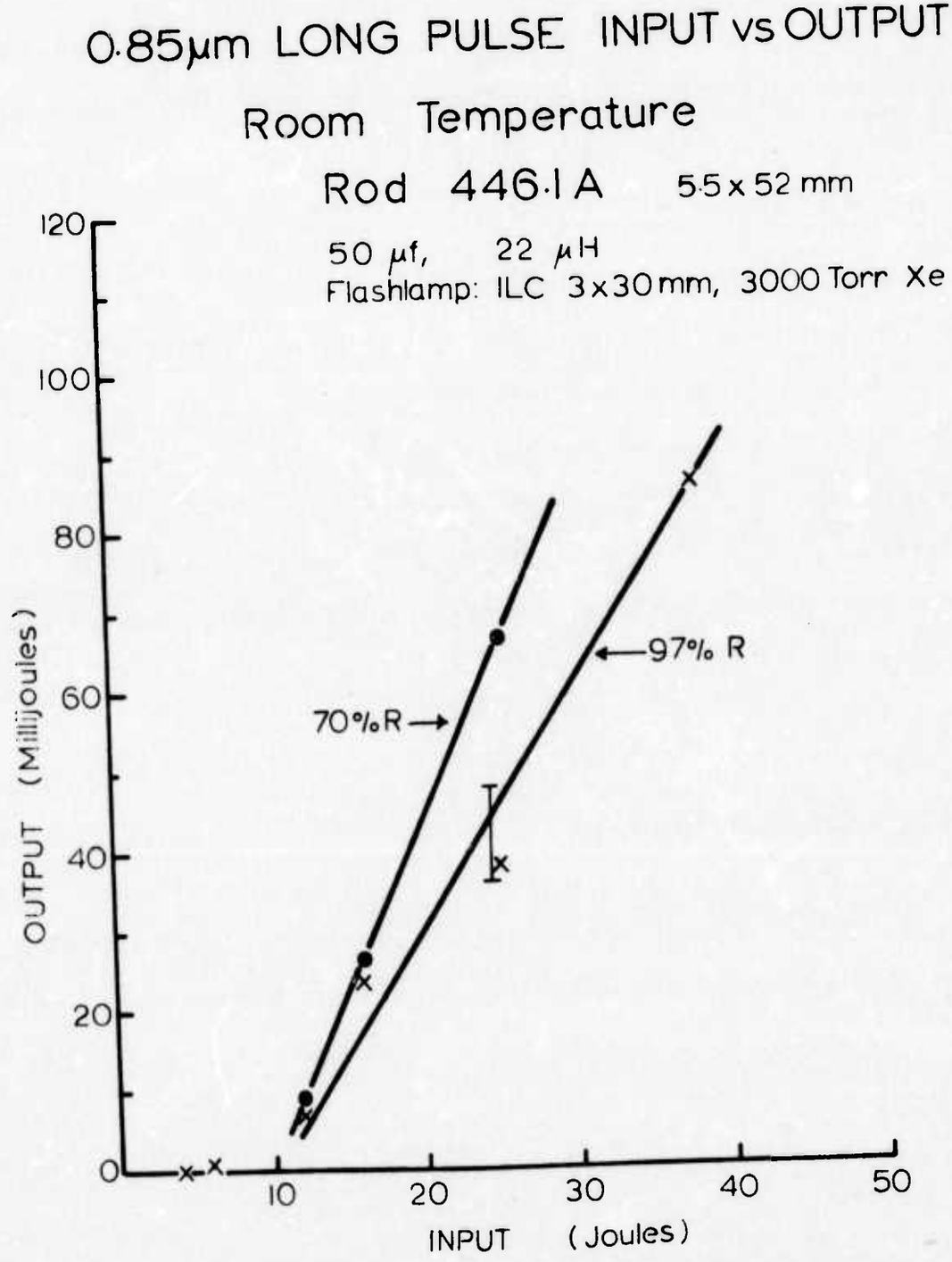
0.85μm LONG PULSE INPUT vs OUTPUT
Room Temperature
Rod 446.1A 5.5x52 mm
50 μf, 22 μH
Flashlamp: ILC 3x30mm, 3000 Torr Xe
120
100
80
60
40
20
0
OUTPUT (Millijoules)
70%R
97% R
10
20
30
40
50
INPUT (Joules)

Figure 4

D-69

where R_1 R_2 = reflectivities of the resonator mirrors

$\alpha = (N_i - N_f)\,\sigma$, the threshold gain

N_i = initial state population density

N_f = terminal state population density

σ = stimulated emission cross-section (cm^2)

Δ = total internal loss coefficient/$_{cm}$

or

$$N_i = \frac{1}{\sigma}\left[\frac{1}{2\ell}\,\ell n\,\frac{1}{R_1R_2} + \Delta\right] + N_f$$

N_f is the population of the terminal level in the $^4I_{13/2}$ manifold at threshold. An upper limit of the thermalized population of this level (N_f^T) is estimated assuming the ground and first excited manifolds are single states separated by 6600 cm^{-1}. Then, an upper bound for the terminal level thermalized population is

$$N_f = N_o \exp\,(-6600/207) = 3.2 \times 10^{-14}\,N_o.$$

For 2% Er YLF $N_o = 3.2 \times 10^{20}$ ions/cm^3, thus $N_f^T \simeq 1 \times 10^7 cm^{-3}$.

For reasonable values of $\Delta(.02cm^{-1})$ and $\sigma(10^{-19}cm^2)$

$$\Delta/_o >> N_f^T,$$

and N_f^T can be neglected.[14]

However, the terminal level is pumped by the flashlamp via direct absorption and by relaxation from higher lying states. The optically pumped terminal level population (N_f^P) cannot be estimated accurately. Since the terminal level lifetime is long, the lower

level population at threshold cannot be ignored. Thus we have

$$N_i = \frac{1}{\sigma}\left[\gamma_R + \Delta\right] + N_f^P$$

where $\gamma_R = \frac{1}{2\ell} \ln \frac{1}{R_1 R_2}$

N_f^P = optically pumped terminal state population at threshold

We assume

$$N_i = AE_t$$

$$N_f^P = BE_t$$

where E_t is energy into the flashlamp at threshold and A and B are constants. Because lasing is observed in this material A must be greater than B. Substituting and rearranging we obtain

$$E_T = \frac{1}{(A-B)\sigma}\left[\gamma_R + \Delta\right]$$

Following Findlay and Clay[12], at zero output coupling ($R_1R_2 = 1$, $\gamma_R = 0$) we have:

$$E_{to} = \frac{\Delta}{(A-B)\sigma}$$

$$E_T = E_{t_o}\left[1 - \frac{\ell n R}{2\ell\Delta}\right]$$

which is identical to the result for a four-level laser with a negligible optically pumped terminal level population (Nd glass or YAG). The scattering loss, Δ, is obtained by plotting the threshold energy vs $-\ell nR$; the measured slope of the line (m) is

$$\frac{E_{t_o}}{2\ell\Delta} = m$$

and E_{t_o} is obtained by extrapolating the plot to zero output coupling.

Laser measurements were made with rod 446.1a (5.5 x 52 mm). The onset of oscillation was monitored (with a Varoscope) as a function of coupling mirror reflectivity. Care was exercised to assure that the data represented the effects of mirror reflectivity alone. The onset of spiking could be reliably determined to ± 10% of the computed energy. The input energy ($1/2\ CV^2$) was computed from a careful measurement of the supply voltage.

The reflectivity of the mirrors was determined with transmission measurements at normal incidence on a Cary 14 at 0.85 μm. Because the laser rod was not AR coated, the rod faces and the mirrors constitute a Fabry-Perot resonator altering the coupling mirror reflectivity.[13] The effective reflectivity for a Fabry-Perot cavity with unequal reflectivities is given by[15]

$$R^1 = \frac{(\sqrt{r} + \sqrt{R})^2}{(1 + \sqrt{r}\,R)^2}$$

where R = the measured coupling mirror reflectivity

r = the normal incidence reflectivity at 0.85 μm of Er^{3+}:YLF

To obtain r the index of refraction data of Shand[4] was extrapolated to 0.85 μm. The extrapolated values are

$$n_o \simeq 1.441\ (\sigma)$$

$$n_e \simeq 1.461\ (\pi)$$

with corresponding reflectivities

$r_o = 0.033$

$r_e = 0.035$

at normal incidence.

Figure 5 shows a plot of the threshold observed with rod 446.1a vs $-\ell nR^1$ (using r = 0.034) from which a loss coefficient

$$\Delta = 0.01 \pm 0.001 cm^{-1}$$

A 1%/cm scattering loss indicates a fairly high quality material. However, visual examination of the rod revealed many bands of small bubbles visible without magnification. Since the measurement of Δ involves a measurement γ at threshold where only filamentary lasing may occur throughout regions of low scattering loss, it is possible that the loss coefficient in the bulk material might be somewhat higher.

5.1.2 ROD 448 2%Er - 1% Tm

Preliminary data has been obtained with this rod under the same conditions described above. Lasing threshold was observed at 10 joules; however at 30J only 4mj was obtained. The optical quality of this rod was "qualitatively equivalent" to 446.1a, above. The poor lasing performance is attributed to the presence of Tm^{3+} which quenches the upper laser level (lifetime 90 μs compared to 220 μs in 2% Er).

5.2 REPETITIVELY PULSED DATA

Repetitively pulsed data was taken in water cooled pump cavities using 3 and 5.5 mm 2% Er rods. In a previous report[1] the output was observed to extinguish after only a few seconds at 10 Hz. A constriction in the coolant line was found to have stopped the water flow. With adequate water flow, > 0.1 gal/min, this behavior did not occur.

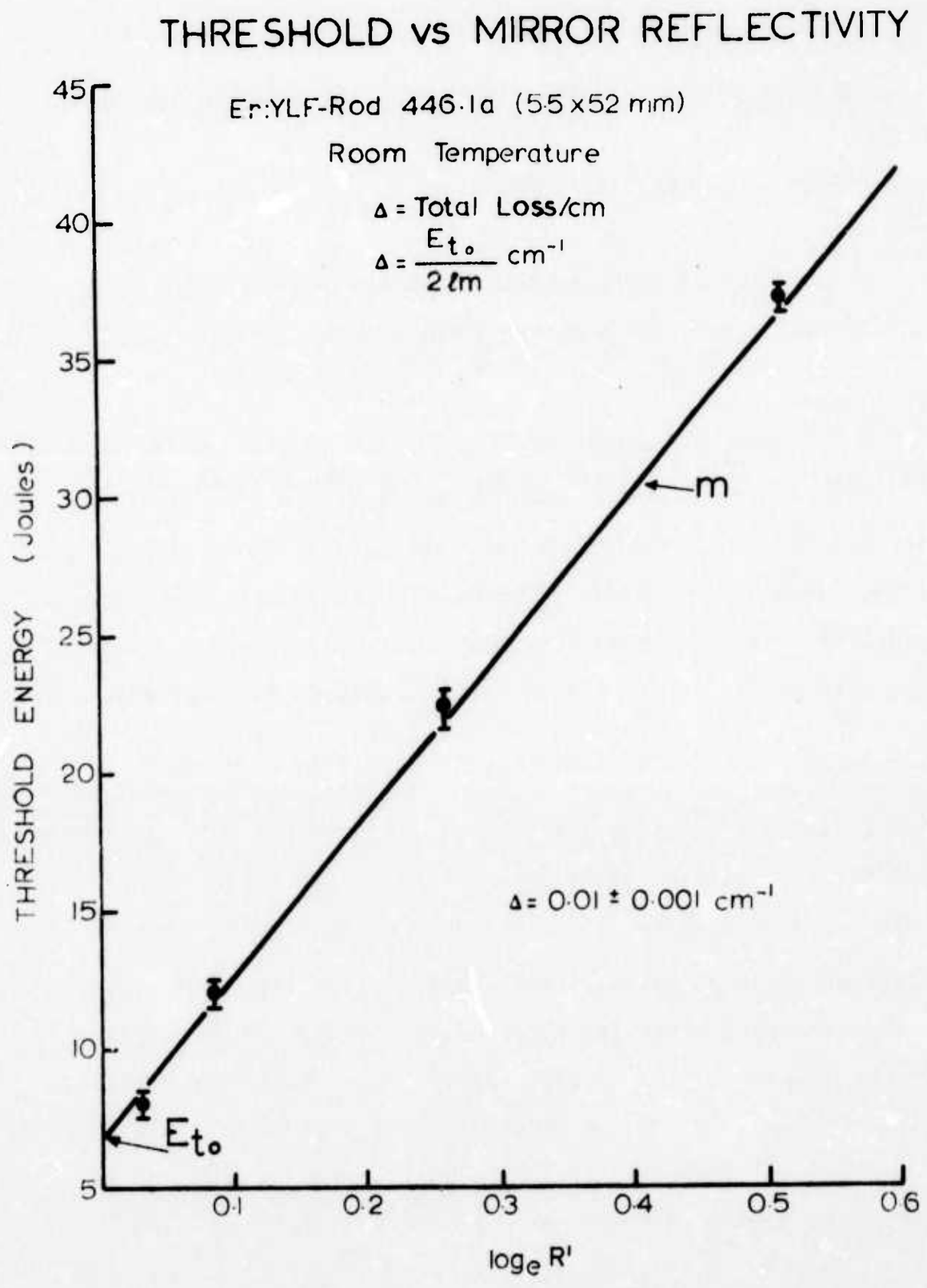
THRESHOLD vs MIRROR REFLECTIVITY
Er:YLF-Rod 446-1a (5.5 x 52 mm)
Room Temperature
Δ = Total Loss/cm
Δ = Et₀ / 2ℓm cm⁻¹
THRESHOLD ENERGY (Joules)
45
40
35
30
25
20
15
10
5
m
Et₀
Δ = 0.01 ± 0.001 cm⁻¹
0.1
0.2
0.3
0.4
0.5
0.6
log_e R'

Figure 5

D - 74

5.2.1 ROD 446.2, 2% Er (3 x 23 mm)

Long pulse operation at 20 pps was obtained under the following conditions:

Flashlamp:	ILC 3000 Torr 3 x 30 mm
Laser Rod:	446.2 2% Er^{3+}:YLF 3 x 37 mm (Uncoated), 23 mm exposed
Pump Cavity:	Silvered cylinder radius = 0.38", length = 1.5"
Flashlamp/Rod Separation:	0.436"
Cooling:	Distilled water flooding the cavity Flow rate ∿ 1 gal/min
Energy Bank:	C = 50 μf, L = 46 μH
Trigger Mode:	Parallel to cavity; EGG TM-11
Resonator:	Plane parallel, L ∿ 0.5 meters
Rod Holders:	Stainless - approximately 15 mm of rod shadowed
Radiometry:	Scientech 3620 Energy/Power Meter

Preliminary measurements were made with a 90% R output mirror; lasing threshold was 7 joules. Repetitively pulsed operation was obtained at 20 pps with 30 mW average power. The input power was not measured.

Measurements were made at 4.2°C and 10°C with the input power monitored by directly observing the changing voltage in an oscilloscope (input power = 1/2 CV^2 x rep. rate). The output mirror reflectivity was 90% R. At 4.2°C, 40 mW were obtained at 20 pps with 16J/pulse (320 watts input). In single shot operation 3 ± 1 mJ was obtained at 16J input. At 10°C, the same results (within ± 10%) were obtained. Experiments at fixed input energy/pulse (16 joules) indicated that the average power output was nearly equal to the single shot

output energy times the pulse repetition rate. Note that the experimental error in the energy measurements at low output energies (<10 mJ) is quite high due to drift in the energy meter.

The output was visually monitored with a Varoscope viewing a target ~ 10 meters from the exit aperture. The spot size was approximately the same as the He-Ne alignment laser (divergence < 1 mr) whose exit aperture was approximately the same distance from the target. The .85 spot size was not observed to change with repetition rate.

No evidence of the saturation effects previously reported[3] were observed. Higher repetition rates were not attempted as the average power dissipation capabilities of the flashlamp were not known. Operation at 30 mW at 20 pps for 2 hours continuously was obtained with no degradation of the output observed.

5.2.2 ROD 446.1a, 2% Er, 5.5 x 52 mm

Repetitively pulsed operation at up to 33 pps was obtained under the following conditions:

Rod:	446.1a, 5.5 x 52 mm, 2% Er
Cavity:	Cylindrical Ellipse (silvered) L = 75 cm, a = 33, b = 29 mm
Flashlamp:	ILC 3 x 50, 3000 Torr Xe
Bank:	C = 50 μf, L = 100 μh
Resonator:	Plane parallel, length = 50 cm
Cooling:	Distilled water - separate coolant loops (pyrex jackets) over rod and lamp, flow rate over rod 1.5 gal/min

With a 97% R lasing threshold was below 16 joules (800V) - the

flashlamp would not fire below this level. The output energy at this input was ~ 1 mJ. With the power supply set at 800V, operation at 20 pps was obtained, although at 20 pps, the actual voltage (measured with a high voltage probe) was about 760 volts. At 36 joules input, only 75 mW were obtained at 20 pps (97% R). In a separate experiment, operation at 33 pps was obtained at ~ 30 joules/pulse input - this upper limit in repetition rate determined by the average power capabilities of the power supply.

A maximum of 250 mW was obtained at 11 pps with 80 joules/pulse input (95% R). The average power output was approximately the energy observed in single shot (at the same pumping level, 3X threshold) X the repetition rate.

The relatively low energy/pulse output was, at first, puzzling in view of previous data which had been obtained with this rod in a more efficient pumping cavity (See Figure 4). Figure 6 shows the input/output characteristics in single shot operation taken in the cooled cavity after the repetitively pulsed experiments indicating far poorer slope efficiencies. The poorer efficiency is due partly to the lower pumping efficiency of the cavity and an apparent increase in the number of scattering inclusions of the rod observed after the repetitively pulsed experiments. Similar behavior was observed with this rod in single shot operation; in this case the output dropped after only a few shots in long pulse. Performance was restored after part of the rod which had developed bands of inclusions was cut off and the rod refabricated. This behavior has <u>not</u> been observed in any other Er^{3+}:YLF rod.

Pumping efficiency in these data was low due to the cavity ineffi-

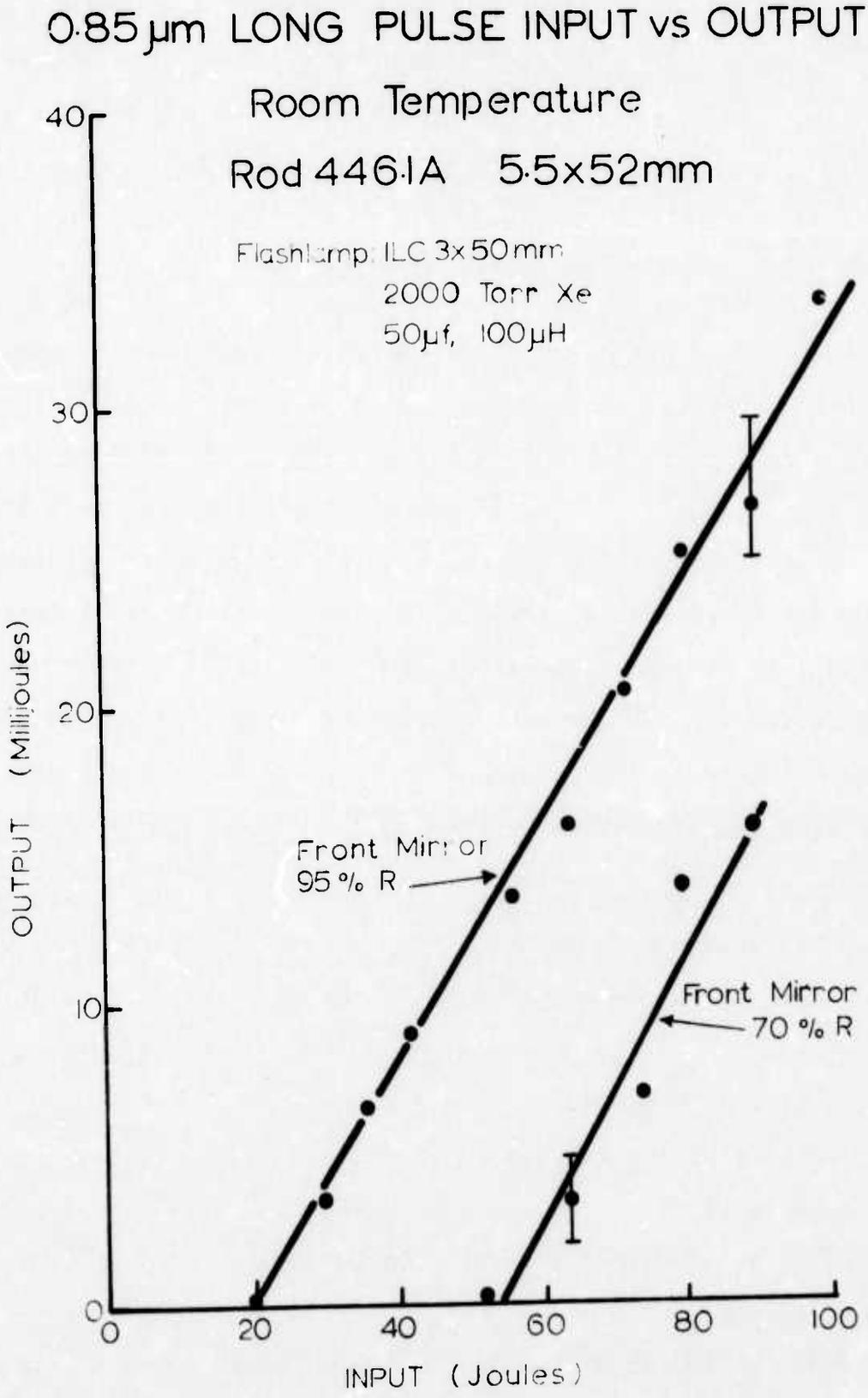
0.85 μm LONG PULSE INPUT vs OUTPUT
Room Temperature
Rod 446-1A 5.5x52mm
Flashlamp: ILC 3x50mm
2000 Torr Xe
50μf, 100μH
Front Mirror
95 % R
Front Mirror
70 % R
OUTPUT (Millijoules)
INPUT (Joules)
0
10
20
30
40
0
20
40
60
80
100

Figure 6

D-88

ciency and the use of pyrex/water jackets which mark some of the near ultra violet pump bands. Obtaining higher average power was limited by lamp loading constraints. Thermal fracture of the rod did not occur.

5.3 LASER POLARIZATION AND Q SWITCHING

5.3.1 POLARIZATION

The polarization of the output was measured with a calcite Glan prism mounted internal and external to the cavity resenator. Pump conditions were identical to those described in 5.2.1. Polarization measurements made external to the cavity in long pulse revealed two maxima separated by 180°. At the transmission minimum (90° from the maximum) some residual spiking was observed probably due to scattered light. With the prism mounted internal to the cavity, oscillations were observed only in two orientations 180° apart at up to 2 x the threshold observed for the optimum orientation. Upon removal of the rod, the polarization vector was found to be parallel to the $\hat{C}$ axis, as expected from the fluorescence spectrum.

5.3.2 Q-SWITCHING

Q-switched outputs were obtained in the above geometry with the resonator extended to accomodate the prism and KDP. The operating parameters were:

1/4 Wave Voltage:	9.7 KV
Electrical Pulse Risetime:	∿ 10 ns
Recovery Time:	∿ 100 ms
Resonator Length:	0.6 meters
Output Reflectivity:	4.5% T at 0.85 μm

Q-switched outputs were first obtained at ∿ 40 joules input at up to 5 pps (only 4 mW output). Typical pulsewidths were 50 - 100 ns at FWHM for single pulses. Superposed multiple pulses (two) were observed in some shots with combined halfwidths of ∿ 150 ns. In repetitively Q-switched operation, only 5 pps (4 mW) could be obtained without exceeding the average power dissipation capabilities of the flashlamp. Input energy/pulse was 40 joules for ~ 1 mj output. Peak power outputs observed were ~ 0.2 MW.

Without the polarizer in the cavity, long pulse oscillations were held off (Q-switch voltage on, not switched) at up to 2 x threshold. Q-switched pulses were obtained without the polarizer, however, in some cases, after pulsing was observed. The after pulses exhibited the amplitude and width characteristics of long pulse spikes.

In separate experiments, the effects of the cavity components on threshold were studied. With an open resonator, threshold was 7.5 joules; addition of the polarizer (with unknown reflectivity at 0.85) increased the threshold to 12 joules in the optimum orientation. With the polarizer and the KDP (no voltage), threshold was 13 joules. Q-switched threshold was 23 joules. Laser damage was not observed in the rod or any of the components. Q-switched performance was limited by losses in the KDP cell (previously damaged on another program) and the calcite polarizer (AR coated at 2.06 μm).

REFERENCES

1. E.P. Chicklis and C. S. Naiman, "Stimulated Emission at 0.85μm in Er^{3+}:YLF", Talk given at VIII International Quantum Electronics Conference, Montreal, May 8, 1972.

2. E.P. Chicklis and C.S. Naiman, Talk given at 1st European Electro-Optics Markets and Technology Conference, Geneva, 13-15 Sept. 1972.

3. V. Belruss, T. Kalnajs and A. Linz, Mat. Res. Bull., Vol. 6, pp. 899-906, 1971.

4. E.P. Chicklis, R.C. Folweiler, C.S. Naiman, A. Linz, H.P. Jenssen, D.R. Gabbe, "Development of Multiply Sensitized Ho:YLF as a Laser Material", TR ECOM-00013-F, ARPA Order No. 1868, Contract No. DAAB07-71-C-0013, January 1973.

5. E.P. Chicklis, R.C. Folweiler, C.S. Naiman, A. Linz, H.P. Jenssen, D.R. Gabbe, " .85 Micron Solid State Laser Material Evaluation", AFAL-TR-73-94, Contract No. F33615-72-C-2065, April 1973.

6. General Electric Co. Space Technology Products, Data Sheet.

7. R. T. McIntyre, IEEE Transactions on Electron Devices, ED-17, 4, pp. 347-352, April 1970.

8. RCA, Electro-Optics Handbook.

9. R. L. Remski, Air Force Avionics Lab., AFAL/TEO, Private Communication.

10. M. R. Brown et. al., J. Phys. C. (Solid State Phys.) 2, 593, (1969).

11. Takashi Kushida, H. M. Marcos and J. E. Gensic, Phys. Rev. 167, 2, pp. 289-291, March 1968.

12. M.J. Weber, Ratheon Company, Research Division, Unpublished.

13. D. Findlay and R.A. Clay, Phys. Letters, 20, 3, pp. 277-278, 1966.

14. D.W. Goodwin, Phys. Letters, 24A, 5, pp. 283-284, (1967).

15. M. Born and E. Wolf, Principles of Optics (Pergamon Press, 1959), p. 324.

APPENDIX I

STRENGTH MEASUREMENT(+)

The strength of αβYLF has been re-measured using a group of samples that were prepared in a manner to minimize the effect of surface damage. The samples were cut from boule 140f and finished by lapping with diamond abrasive. A final chemical polish of Syton* was used to leave a damage free surface on the side that was to be placed in tension during the test. An attempt was made to chamfer the tension edges, but difficulties were encountered in the procedure.

Surface microcracks and scratches are known to reduce the observed strength of all materials tested in tension, but their effect is greatest on materials that have little plastic flow before fracture. A scanning electron microscope was used to examine the tension surface of samples 2 and 3 after completion of the strength measurements. Very little cracking was observed anywhere, although the fracture surfaces did appear to originate from flaws at the edges that probably existed prior to testing. The tension surface of sample 3 was of such high quality that it was very difficult to focus the microscope on it at

---

+Work performed under ARPA Order No. 1868, Contract No. DAAB07-73-C-0066
*T-M-Monsanto Co.

63000X without the aid of a small scratch or dust particle. Sample 2 showed some surface pits, indicating that it was not as well polished.

The strength was measured in an Instrom testing machine using a carefully aligned four-point test fixture. Sample dimensions were approximately 0.06 inches thick by 0.19 inches in breadth. The modulus of rupture was calculated using the formula

$$\sigma_f = \frac{3P(c-a)}{2bT^2}$$

where σ_f = modulus of rupture

P = load at fracture

c = distance between outer load points

a = distance between inner load points

b = specimen width

and T = specimen thickness

The observed strength of the samples is shown in Table A-I. All samples broke between the inner load points.

The data represents reasonably low scatter for strength measurements.

TABLE A-I

STRENGTH OF αβYLF

Composition $Li\ Y_{0.34}\ Er_{0.50}\ Tm_{0.067}\ Ho_{0.0034}\ F_4$

Boule 140f

SPECIMEN	STRENGTH psi
1	4630
2	4250
3	5500
4	4650
Average	4760

(9) Semi-annual rept. no. 2, 5 Dec - 5 Jun 73,

UNCLASSIFIED
Security Classification

DOCUMENT CONTROL DATA - R & D

(Security classification of title, body of abstract and indexing annotation must be entered when the overall report is classified)

1. ORIGINATING ACTIVITY (Corporate author)
Sanders Associates, Inc.
95 Canal Street
Nashua, New Hampshire 03060

2a. REPORT SECURITY CLASSIFICATION
Unclassified

2b. GROUP
N/A

3. REPORT TITLE
(6) 0.85 Micron Solid State Laser Material Evaluation, Part II.

4. DESCRIPTIVE NOTES (Type of report and inclusive dates)
[redacted] Technical Report, 5 Dec [redacted] - 5 Jun [redacted]

5. AUTHOR(S) (First name, middle initial, last name)
(10) Evan P. Chicklis, Robert C. Folweiler, Charles S. Naiman, et al

6. REPORT DATE
(11) Oct [redacted] 73

7a. TOTAL NO. OF PAGES
~~48~~ (12) 53 b.

7b. NO. OF REFS
15

8a. CONTRACT OR GRANT NO.
(15) F33615-72-C-2165, ARPA Order-2075

b. PROJECT NO.
~~2075~~ See "Foreword"

c.

d.

9a. ORIGINATOR'S REPORT NUMBER(S)
N/A (18) AFAL

9b. OTHER REPORT NO(S) (Any other numbers that may be assigned this report)
N/A (19) TR-73-94-Pt-2

10. DISTRIBUTION STATEMENT
Distribution limited to United States Government Agencies only; by reason of inclusion of test and evaluation data; applied October 1973. Other requests for this document must be referred to AFAL/TEO, Wright-Patterson AFB, Ohio 45433.

11. SUPPLEMENTARY NOTES

12. SPONSORING MILITARY ACTIVITY
Advanced Research Projects Agency
Materials Science Directorate
1400 Wilson Blvd., Arlington, Va. 22209

13. ABSTRACT
This second semi-annual report describes the current status of the program for the development of a room temperature, 0.85 micron optically pumped laser material, Er:YLF. Substantial progress has been made in defining the physical, spectroscopic and laser characteristics of this material. The measured value of the stimulated emission cross section is ~~1.5×10^{-19} cm^2~~. Laser oscillations in this material are predominantly π polarized. Long pulse operation at up to 33 pps is reported. The maximum observed output power was of 0.25 watts at 11 pps from a 5.5 x 52 mm 2% Er rod.

* 1.5 x 10 to the -19th power sq cm.

406 141

DD FORM 1 NOV 65 1473 REPLACES DD FORM 1473, 1 JAN 68, WHICH IS OBSOLETE FOR ARMY USE.

UNCLASSIFIED
Security Classification

14 KEY WORDS	LINK A ROLE	LINK A WT	LINK B ROLE	LINK B WT	LINK C ROLE	LINK C WT
0.85 Micron Laser						
Laser Material Evaluation						
Er:YLF						
Erbium						
Stimulated Emission						
Top Seeded Solution Technique						
Four Level Laser						
Optically Pumped Laser						
Lithium Yttrium Fluoride						
YLF						
IR Laser						